10.18605/2175-7275/cereus.v17n4p395-410

ARTIGO ORIGINAL

<< Recebido em:25/03/2025 Aceito em: 20/06/2025 . >>

REVISTA CEREUS ISSN: 2175-7275

Assessing the Impact of Anisotropic Hydraulic Conductivity on Lateral Flow for Streamflow Predictions in a Representative Atlantic Forest Watershed

Avaliação do Impacto da Condutividade Hidráulica Anisotrópica no Fluxo Lateral para Previsões de Vazão em uma Bacia Representativa da Mata Atlântica

Dhiego da Silva Sales[1], Jader Lugon Junior[2], David de Andrade Costa[3], Ana Oliveira[4], Debora Pereira[5], Ramiro Neves[6], Antônio José da Silva Neto[7]

ABSTRACT

The anisotropy of soil introduces considerable uncertainty due to factors like soil formation processes, management practices, and spatial variability. This heterogeneity poses challenges in accurately determining anisotropy values for watersheds modeling, often necessitating a trial-and-error approach. This study investigates the effects of anisotropic hydraulic conductivity on streamflow dynamics using the MOHID-Land model, with a focus on achieving efficient soil calibration and enhancing streamflow predictions in a representative Atlantic Forest watershed. By simulating different anisotropy ratio values, the study analyzes hydrograph characteristics through the Nash-Sutcliffe Efficiency (NSE) metric. Results indicate that increasing anisotropy ratio flattens the hydrograph, dampening flow peaks while elevating base flow. This non-linear relationship reaches an improved point before declining, suggesting the existence of a watershed-specific anisotropy value that maximizes predictive accuracy.

Keywords: Soil Physics. Hydrologic Modeling. Porous Media. Mass Transport. Water Resource Management.

RESUMO

A anisotropia do solo introduz considerável incerteza devido a fatores como processos de formação do solo, práticas de manejo e variabilidade espacial. Essa heterogeneidade apresenta desafios na determinação precisa dos valores de anisotropia para modelagem de bacias hidrográficas, muitas vezes necessitando de uma abordagem de tentativa e erro. Este estudo investiga os efeitos da condutividade hidráulica anisotrópica na dinâmica do fluxo de água usando o modelo MOHID-Land, com foco em alcançar calibração eficiente do solo e melhorar as previsões de fluxo de água em uma bacia hidrográfica representativa da Mata Atlântica. Ao simular diferentes valores de razão de anisotropia, o estudo analisa as características do hidrograma por meio da métrica de eficiência de Nash-Sutcliffe (NSE). Os resultados indicam que o aumento da razão de anisotropia achata o hidrograma, amortecendo os picos de fluxo enquanto eleva o fluxo de base. Essa relação não linear atinge um ponto ótimo antes de declinar, sugerindo a existência de um valor de anisotropia específico da bacia hidrográfica que maximiza a precisão preditiva.

Palavras-chave: Física do Solo. Modelagem Hidrológica. Meios Porosos. Transporte de Massa. Gestão de Recursos Hídricos.

[1] Doutor em Modelagem e Tecnologia para Meio Ambiente Aplicadas em Recursos Hídricos pelo IFF. Orcid: https://orcid.org/0000-0001-6541-4720. E-mail: dhiego.sales@outlook.com

[2] Doutor em Modelagem Computacional pela UERJ e professor no IFF. Orcid: https://orcid.org/0000-0001-8030-0713. E-mail: jlugonjr@gmail.com

[3] Doutor em Planejamento Energético pela COPPE/UFRJ e professor no IFF. Orcid: https://orcid.org/0000-0003-1814-5892. E-mail: david.costa@gsuite.iff.edu.br

[4] Doutora em Engenharia Ambiental pelo IST/Universidade de Lisboa. Orcid: https://orcid.org/0000-0001-9760-5783. E-mail: anaramosoliveira@tecnico.ulisboa.pt

[5] Mestra em Geofísica pela UFPA. Orcid: https://orcid.org/0000-0003-2085-6570. E-mail: debora.pereira@tecnico.ulisboa.pt

[6] Doutor em Ciências Aplicadas pela Université de Liège. Orcid: https://orcid.org/0000-0001-6571-5697. E-mail: ramiro.neves@tecnico.ulisboa.pt

[7] Doutor em Engenharia Mecânica pela North Carolina State University. Orcid: https://orcid.org/0000-0002-9616-6093. E-mail: ajs_neto@uol.com.br

1. INTRODUCTION

The infiltration of water into soil is predominantly governed by the Richards Equation, a nonlinear parabolic partial differential equation that captures the transient flow of water through porous media, moving from zones of higher to lower pressure (RICHARDS, 1931). A crucial parameter in this process is hydraulic conductivity, which dictates the rate of water movement into the soil. Higher hydraulic conductivity accelerates infiltration and drainage rates (USOWICZ & LIPIEC, 2021). Under unsaturated conditions, hydraulic conductivity is intricately linked to the Soil Water Characteristic Curve (SWCC), a key relationship that defines how soil moisture affects conductivity. The SWCC is commonly modeled by empirical equations, with the van Genuchten (1980) model being among the most widely applied. By assessing the SWCC, researchers can estimate hydraulic conductivity across varying soil moisture levels, providing critical insights for predicting infiltration rates and drainage behaviors.

Hydraulic conductivity frequently displays directional variability, with distinct values along vertical and horizontal planes. In isotropic soils, conductivity is uniform across all directions; however, in anisotropic soils, conductivity differs by orientation – typically showing higher rates horizontally than vertically, which facilitates lateral flow over vertical infiltration Anisotropy arises from soil formation processes, particle alignment, and stratification, often favoring horizontal over vertical water movement (WOESSNER & POETER). This directional preference plays a crucial role in hydrological processes, especially in sloped terrains where lateral flow can enhance downslope water movement, influencing streamflow and groundwater recharge (BECK-BROICHSITTER et al., 2022).

Horn et al. (2020) argue that anisotropy is also influenced by both intrinsic soil properties and anthropogenic impacts such as compaction from agricultural machinery, trampling by livestock, and other management practices. These disturbances further increase the uncertainty of accurately estimating the anisotropy ratio, complicating efforts to apply these estimates across larger spatial domains, such as watersheds.

Given the analytical complexity of solving the Richards Equation, hydrological models that employ numerical methods are often preferred for practical applications. The MOHID-Land model was selected for this study due to its robust, open source, physically based, spatially distributed framework, which applies finite volume methods to solve the mass and

momentum conservation equations (OLIVEIRA et al., 2020). Within the MOHID-Land platform, hydraulic conductivity anisotropy is managed via a multiplier known as the K_Factor (KF), with a value of 1 indicating isotropy and values different of 1 reflecting varying degrees of anisotropy (positive or negative).

The Pedro do Rio watershed in Petrópolis, located in the mountainous region of Rio de Janeiro, was chosen as the study area for several reasons. This watershed is a representative example of the Brazilian Atlantic Forest, a high-priority conservation hotspot that plays a critical role in biodiversity preservation, regional climate regulation, and water resource management. Its mountainous terrain makes it particularly sensitive to lateral flow dynamics, where anisotropy in soil hydraulic properties could significantly impact flow patterns. Moreover, previous studies have highlighted the challenges associated with modeling porous media fluxes in this area, especially regarding the accurate representation of lateral flow in particular during low flow conditions (ARAUJO, 2026; VILLAS-BOAS, 2018).

Given the study area's steep topography, we assumed that lateral flow is a crucial hydrological process. We assume a positive anisotropy ratio, indicative of preferential lateral flow, as the basis for our analysis. The absence of studies quantifying the sensitivity and uncertainty of anisotropy in the MOHID-Land model represents a notable gap, which this study seeks to address. By focusing on the Pedro do Rio watershed, this research seeks to advance the understanding of hydrological processes in mountainous regions of the Atlantic Forest biome and contribute to the refinement of models that could be applied to other areas with similar characteristics.

2. MATERIALS AND METHODS

2.1 Study Area

Pedro do Rio is a representative watershed covering around 420 km² and is located in Petrópolis, within the mountainous region of Rio de Janeiro. This watershed was delineated as part of the project Integrated Studies in Experimental and Representative Basins (EIBEX), one of Brazilian Geological Service (CPRM) ongoing initiatives in Brazil focused on long-term watershed monitoring in key biomes. EIBEX-selected watersheds represent broader watershed characteristics based on physical, environmental, economic, and social factors (Villas-Boas et al., 2017). Additionally, the watershed’s outlet coincides with a fluviometric station managed by the National Water and Sanitation Agency (ANA). This

station also provides observed data that is used to evaluate the model in terms of streamflow values, as illustrated in Figure 1.

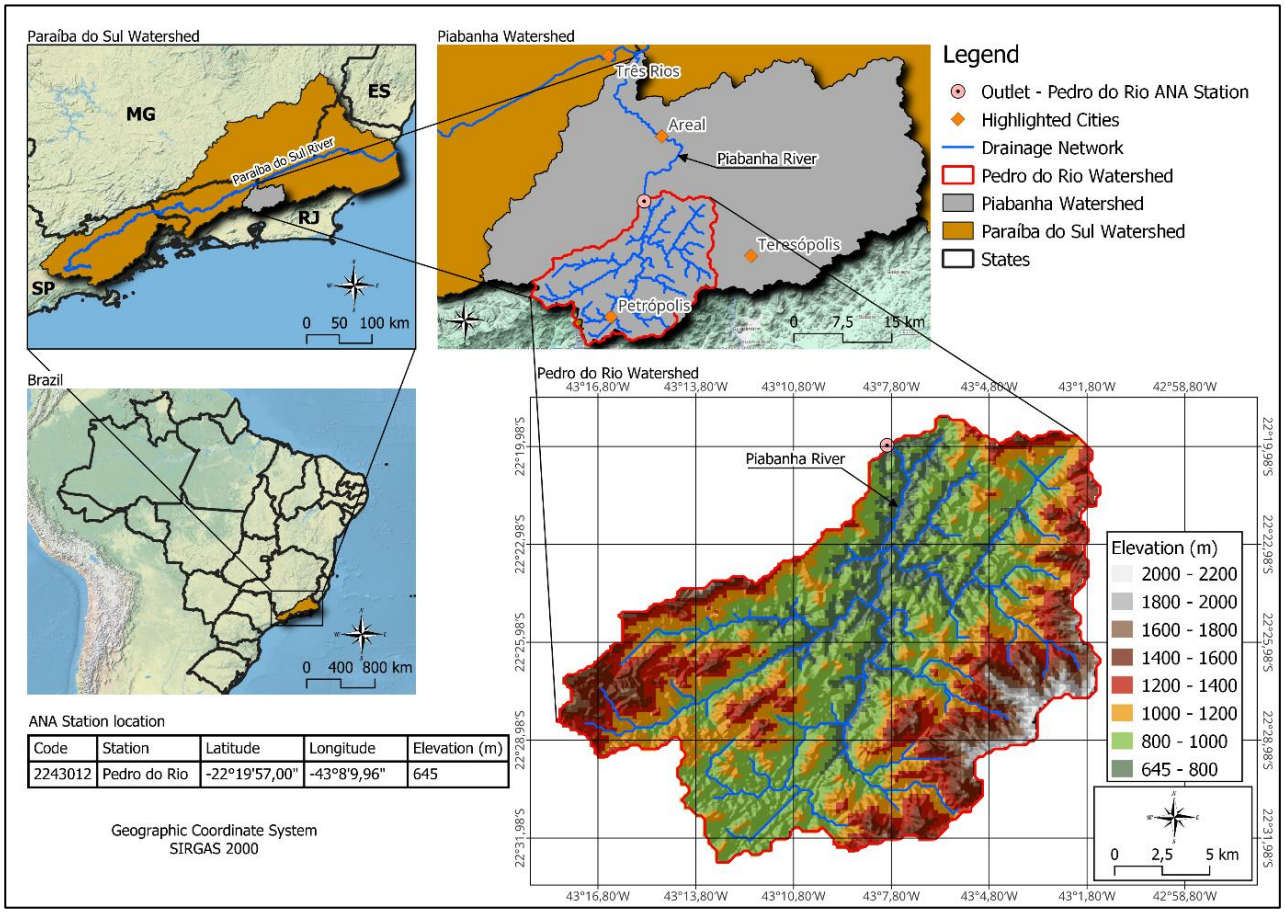

Figure 1. Location of the Pedro do Rio watershed, drainage network, monitoring station and elevation.
Source: prepared by the authors.

The altitude within the region varies significantly, spanning an approximate range of 1450m. This includes elevations that peak at 2200m and descend to a minimum of 645m in the outlet area. The seasons are well defined, and the precipitation distribution is spatially consistent. The higher altitude regions are characterized by a humid tropical climate, where the average annual precipitation exceeds 2000mm. In contrast, the lower regions of the watershed are subject to a subhumid climate, with an average annual precipitation close to 1300mm (COSTA et al., 2021).

2.2 MOHID-Land description

The MOHID-Land model discretizes the domain into finite volumes through horizontal and vertical divisions: the horizontal grid is defined by a spatial resolution specified by the user,

while the vertical layers are divided into fixed or variable thickness layers, also defined by the user, extending to a specified maximum depth. The drainage network is derived from terrain elevation, linking the surface cells centers along flow pathways where flow calculations occur. The Saint-Venant equation governs drainage in the 1D channel network and surface flow in the 2D domain. Atmospheric interactions are not directly simulated; instead, meteorological data are incorporated as boundary conditions.

Infiltration in MOHID-Land is modeled using Darcy's Law, where water movement is driven by pressure gradients and hydraulic conductivity. Under saturated conditions, hydraulic conductivity reaches its maximum value, but as soil moisture decreases, conductivity varies according to the available water content. Water movement in 3D domain is computed by combining the Buckingham-Darcy framework with the continuity equation, resulting in the Richards Equation (Equation 1). To represent soil moisture dynamics, the model employs the SWCC from van Genuchten (1980) and the hydraulic conductivity function from Mualem (1976), as outlined in Equations 2-4. Horizontal conductivity $K_{sat,hor}$ is adjusted using the KF factor, as shown in Equation 5.

$$\frac{\partial \theta}{\partial t} = \frac{\partial}{\partial x_i}\left(K_i(\theta)\left(\frac{\partial H}{\partial x_i}\right)\right) - S(h) \quad (1)$$

$$K(\theta) = K_{sat} \,.\, S_e^L.(1 - (1 - S_e^{1/m})^{\,m})^2 \quad (2)$$

$$S_e = \frac{\theta(h) - \theta_r}{\theta_s - \theta_r} = \left[\frac{1}{1+(\alpha h)^n}\right]^m \rightarrow h = \frac{1}{\alpha}\left(S_e^{\,-1/m} - 1\right)^{-1/n} \quad (3)$$

$$\theta(h) = \theta_r + \frac{\theta_s - \theta_r}{[1+(\alpha|h|)^n]^m} \quad (4)$$

$$KF = {K_{sat,hor}}/{K_{sat}} \quad (5)$$

Where: $K(\theta)$ is the hydraulic conductivity in direction i [m/s], θ is the water content [m³/m³], H is the hydraulic gradient (topography + hydrostatic pressure + suction pressure) [m], x_i is the direction, $S(h)$ is the term for water uptake from the soil by plant roots [m³/s], θ_s is the saturated water content [m³/ m³], θ_r is the residual water content [m³/m³], h is the suction pressure [m], K_{sat} is the vertical saturated conductivity [m/s]; S_e is the effective saturation [dimensionless], α is a curve adjustment parameter, related to the inverse of the air entry [m^{-1}], n is also a curve adjustment parameter, related to the pore size distribution

[dimensionless], m is obtained from relation $1 - 1/n$ (Mualem restriction), *L* is the empirical pore connectivity [m], established in 0.5 (MUALEM, 1976); KF is the hydraulic conductive multiplying factor [dimensionless]; $K_{sat,hor}$ is the horizontal saturated conductivity [m/s].

The soil hydraulic parameters K_{sat}, θ_s, θ_r, n and α can be estimated using pedotransfer functions from the Rosetta model version 3 (ZHANG & SCHAAP, 2017). This model links readily measurable soil attributes – such as clay, silt, and sand fractions, as well as bulk density – to the hydraulic parameters required to characterize the SWCC.

2.3 Model set-up

A regular grid of 200 m was used to cover the entire modeled domain, consisting of 160 rows and 200 columns. The grid's origin (left down corner) is defined by the coordinates 43.36ºW and 22.59°S. The Digital Elevation Model (DEM) utilized, with 30 m spatial resolution, was sourced from the Topodata Project (VALERIANO & ROSSETI, 2012) and subsequently interpolated to match the project's spatial resolution.

Cross-sections for channel geometry were estimated from field monitoring campaigns conducted from 2019 to 2021, organized by the Piabanha Watershed Committee. These cross-sections were modeled as trapezoidal to best approximate the natural streambed profiles with dimensions determined based on the drainage area.

Land use mapping with a 30 m spatial resolution was sourced from the MapBiomas project (SOUZA et al., 2020) and used to classify vegetation types and assign Manning's roughness coefficients, which varied from 0.03 to 0.16 $s/m^{1/3}$. Three vegetation classes – forest, pasture, and agriculture – were identified, allowing for the assignment of crop coefficients (K_c) across growth stages, ranging from 0.6 to 1.0 (ALLEN et al., 1998).

Soil hydraulic parameters were derived from the Rosetta model, utilizing the soil texture database from Brazilian Agricultural Research Corporation (EMBRAPA) (VASQUES et al., 2021a, 2021b), which includes data on sand, clay, silt content, and bulk density. This data was processed with the MOHID SOIL TOOL (SALES et al., 2024), enabling calculation of hydraulic parameters for each soil type within the watershed. The soil domain was then discretized into seven layers, using all six soil horizons provided by EMBRAPA. The maximum soil deep used was seven meters.

Climatic data, including air temperature, wind speed, relative humidity, solar radiation, and cloud cover were obtained from the ERA5 global model. This model supplies hourly

atmospheric data with a 0.25° x 0.25° grid resolution and provides an extensive historical record from 1950 onward (HERSBACH et al., 2020). Daily precipitation data from 39 stations across the watershed were aggregated into 15 synthetic stations through clustering methods based on median values, following Costa et al. (2024). To address gaps in temporal data series, the HyKit tool from UNESCO-IHE (MASKEY, 2013) was used to interpolate missing values based on surrounding stations, weighting for distance and elevation – a necessary adjustment given the significant rainfall variability in the Pedro do Rio watershed's mountainous landscape.

2.4 Uncertainty and error analysis

Error and uncertainty analysis was conducted by individually adjusting the KF parameter in successive simulations while holding all other coefficients constant. The range for KF was set from 1 (representing isotropic soil) up to a maximum of 100, based on Yeh &Tsai's (2018) findings, which indicate that anisotropy ratios range from 2 to 10 for alluvial soils and can exceed 100 for clayey soils. It is notable that the default value for MOHID-Land is 10. The selected range of KF values is summarized in Table 2

Channel flow at the watershed outlet was calculated for each scenario and then compared to observed data. The similarity between modelled and observed streamflow was evaluated using the Nash-Sutcliffe Efficiency (NSE, equation 6) coefficient. This metric evaluates model accuracy by comparing residual variance to the variance of observed data, with values ranging from -∞ to 1. An NSE below 0 suggests that the observed mean provides a better prediction than the model. An NSE of 1 indicates perfect alignment between observed and predicted values (MORIASI et al., 2015). By applying the BIAS metric (Equation 7), it is possible to identify the streamflow response (increase or decrease) to each change in the KF parameter. A positive BIAS indicates that the model overestimates the observed values, while a negative BIAS suggests that the model underestimates them.

$$NSE = 1 - \left[\frac{\sum_{i=1}^{p}(Q_i^{obs} - Q_i^{sim})^2}{\sum_{i=1}^{p}(Q_i^{obs} - Q_{mean}^{obs})^2}\right] \quad (6)$$

$$BIAS = \frac{\sum_{i=1}^{N}(Q_i^{sim} - Q_i^{obs})}{N} \quad (7)$$

where Q_i^{sim} is the simulated flow for day i [m³/s]; Q_i^{obs} is the observed flow on day i [m³/s]; Q_{mean}^{obs} is the observed mean flow for the period [m³/s]; N is the number of observations.

Uncertainty was further evaluated through the 95 Percent Prediction Uncertainty (95PPU) method, which quantifies prediction uncertainty by retaining the central 95% of values, discarding the upper and lower 2.5%. This retained range defines the uncertainty band for all scenarios. A wider band suggests greater model sensitivity to parameter variations, indicating higher uncertainty (ABBASPOUR, 2015). The 95PPU was calculated using the Timeseries Error and Uncertainty Analyzer (SALES et al., 2024).

Table 2. Simulation scenarios for uncertainty analysis.

Simulation	KF	Simulation	KF	Simulation	KF	Simulation	KF
S1	1	S3	10	S5	25	S7	75
S2	5	S4	15	S6	50	S8	100

The analysis simulations were conducted over the period from 2006 to 2008, with 2006 designated as a warm-up period and therefore excluded from the analysis. The following two years were deemed suitable for assessing the impact of parameter variations while optimizing computational cost. This period was divided into a wet season (October to March) and a dry season (April to September), reflecting a typical tropical rainfall distribution.

3. RESULTS

3.1 Streamflow response for KF changes

The BIAS analysis (Figure 2) for the wet season has indicated that the model consistently overestimated the observed streamflow across all tested KF values. This overestimation suggests that the model may place excessive emphasis on rapid hydrological processes, such as surface runoff, while underrepresenting slower processes like percolation. During the dry season, the behavior was more complex. While the model generally underestimated baseflow, an overestimation was observed for $KF = 15$.

A deeper analysis of the relationship between KF and simulated streamflow revealed almost symmetrical behavior across the two seasons. For the wet season, the simulated streamflow decreased with increasing KF values up to a turning point at $KF = 15$, after which the trend reversed. Conversely, in the dry season, simulated streamflow increased until this point and then declined. This pattern indicates a flattening of the streamflow curve.

3.2 Model performance for KF changes

Under isotropic assumptions (S1), a significant portion of the water reaching the soil is swiftly redirected as surface runoff to the river, indicating an imbalance between infiltration capacity and precipitation intensity during periods of high rainfall. This imbalance leads to a marked increase in river peak flow. Conversely, during dry periods, water release from the soil to the river occurs at a slower rate, resulting in reduced base flow due to limited lateral flow. This dual effect – elevated peak flow during intense rainfall and reduced base flow under dry conditions – introduces substantial deviations in the model's hydrograph when compared to simulated and observed data. An NSE value of -2.05 (refer to Table 3) over the full simulation period underscores a poor fit relative to observed data, with similarly low NSE values during both wet (-1.24) and dry (-2.62) seasons. These results suggest that the isotropic condition does not adequately capture real soil-water interactions or river flow dynamics. Therefore, assumptions incorporating anisotropy and enhanced lateral flow modeling may better account for these interactions, leading to improved predictive accuracy.

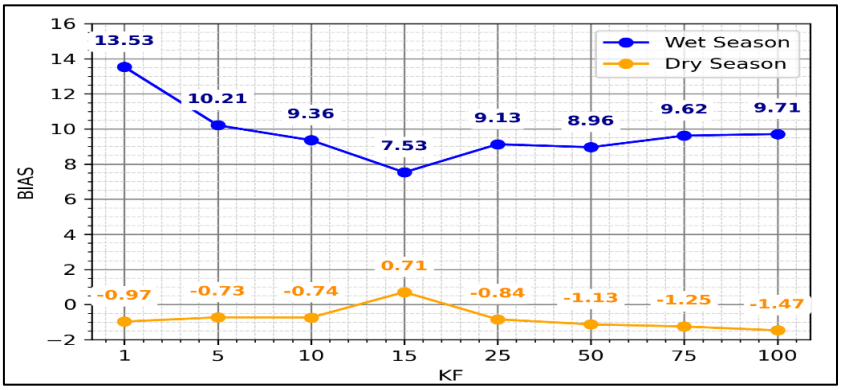

Figure 2. BIAS for wet and dry season during *KF* change.

Table 3. NSE result considering the full period, the wet and the dry season.

KF	NSE			KF	NSE		
	Full Period	Wet Season	Dry Season		Full Period	Wet Season	Dry Season
1	-2.05	-2.62	-1.24	25	0.10	-0.09	0.59
5	-0.28	-0.57	0.51	50	0.17	-0.01	0.64
10	0.01	-0.21	0.60	75	0.09	-0.1	0.63
15	0.33	0.19	0.63	100	0.07	-0.13	0.60

For $KF = 5$, the model demonstrated NSE values of -0.28 for the full period, -0.57 for the wet season, and 0.51 for the dry season. This configuration shows some improvement over the isotropic condition. However, $KF = 5$ still displays a considerable deviation, particularly during the wet season, suggesting that while introducing anisotropy helps, the magnitude of hydraulic conductivity remains inadequate to capture wet season flow peaks effectively.

As KF values increased, there was a notable improvement, especially in the dry season NSE values. For instance, with $KF = 10$, NSE reached 0.60 during the dry season, indicating enhanced performance in base flow conditions. The maximum NSE for the dry season was achieved when $KF = 15$ with a value of 0.65, suggesting an improved representation of soil-water interactions for drier conditions. Beyond this threshold, dry season NSE values stabilized at 0.59–0.64, even with KF increases up to 100, indicating a plateau where further changes in hydraulic conductivity have minimal effect on model performance.

However, during wet season the NSE values remained relatively low across all tested KF levels, reaching a maximum of only 0.19 with $KF = 15$ and subsequently fluctuating around negative values at higher KF settings. This trend implies that while the model performs well under drier conditions with moderate anisotropic settings, it does not fully capture peak flows associated with intense rainfall events, even with higher anisotropy. Of course, this research was limited to testing the variation of a single parameter (KF).

Figure 3 illustrates the non-linear relationship between the NSE and the KF. The results indicate that increasing hydraulic conductivity anisotropy ratio does not necessarily lead to improved model performance. The presence of both a local maximum at $KF = 50$ and a global maximum at $KF = 15$ suggests that there is an improved level of anisotropy for maximizing model accuracy. Consequently, careful attention must be given during the calibration process, as local improvements may occur that do not reflect the globally improved value of KF.

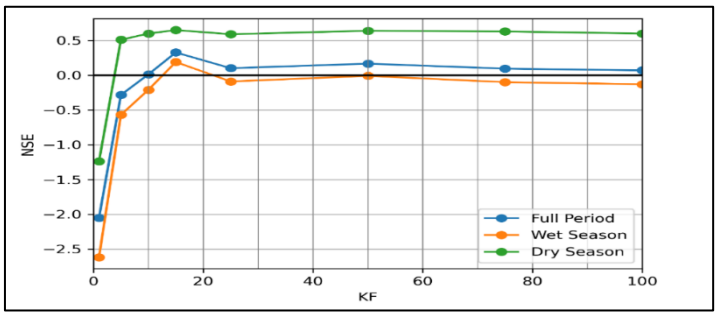

Figure 3. Non-linearity between KF and NSE.

Figure 4 displays the observed and simulated (S4 - $KF = 15$) hydrographs, illustrating a strong alignment in base flow but an overestimation during rainfall periods. This suggests that, while calibrating the KF parameter has notably enhanced the channel flow simulation, further refinement is needed for accuracy during high-flow events. Additional parameters can be used to achieve a more precise representation of the high flow events in the model, such as manning coefficient, grid cell resolution, K_C, cross section area or leaf area index. However, this approach is out of scope of this research.

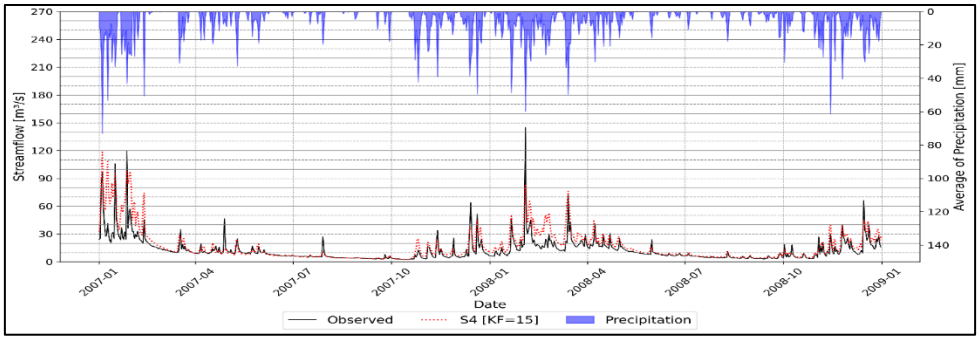

Figure 4. Best performance experiment.

3.3 Uncertainty band for KF changes

MOHID-Land demonstrated high sensitivity to KF values within the range of 1 to 100, as shown by the channel flow uncertainty band (95PPU) in Figure 5a, which reveals substantial fluctuations over time. This variability reflects changes in channel flow and is evident during both drought and rainfall periods, with particularly pronounced effects observed during rainfall events. Based on NSE, a refined exploration of the KF parameter range was proposed, omitting scenarios S1 and S2. Figure 5b reveals that the greatest uncertainty in KF occurs during high-flow periods, where its influence on model dynamics is substantial, notably in attenuating peak flows during rainfall events. However, the impact of KF on flow is minimal during dry periods. The narrower uncertainty band in Figure 5b, compared to Figure 5a, underscores the increased uncertainty associated with KF values in the 1-10 range relative to the 10-100 range.

4. DISCUSSION

The findings of this study corroborate Oliveira et al. (2020), whose sensitivity analysis of the KF parameter highlighted notable improvements in river flow predictions within the range

of 10 to 20. However, their study did not explore KF values beyond this range, leaving a gap in understanding flow behavior under broader anisotropic conditions. Literature on the variation range of the KF parameter remains scarce, with discussions primarily confined to geotechnical studies such as Horn et al. (2020) and Yeh et al. (2018). This underscores the importance of further investigation to enhance the predictive accuracy and reliability of river flow modeling. By expanding the analysis to a broader range of KF values, this study offers critical insights into river flow dynamics. It deepens our understanding of the implications of KF variability in hydrological modeling.

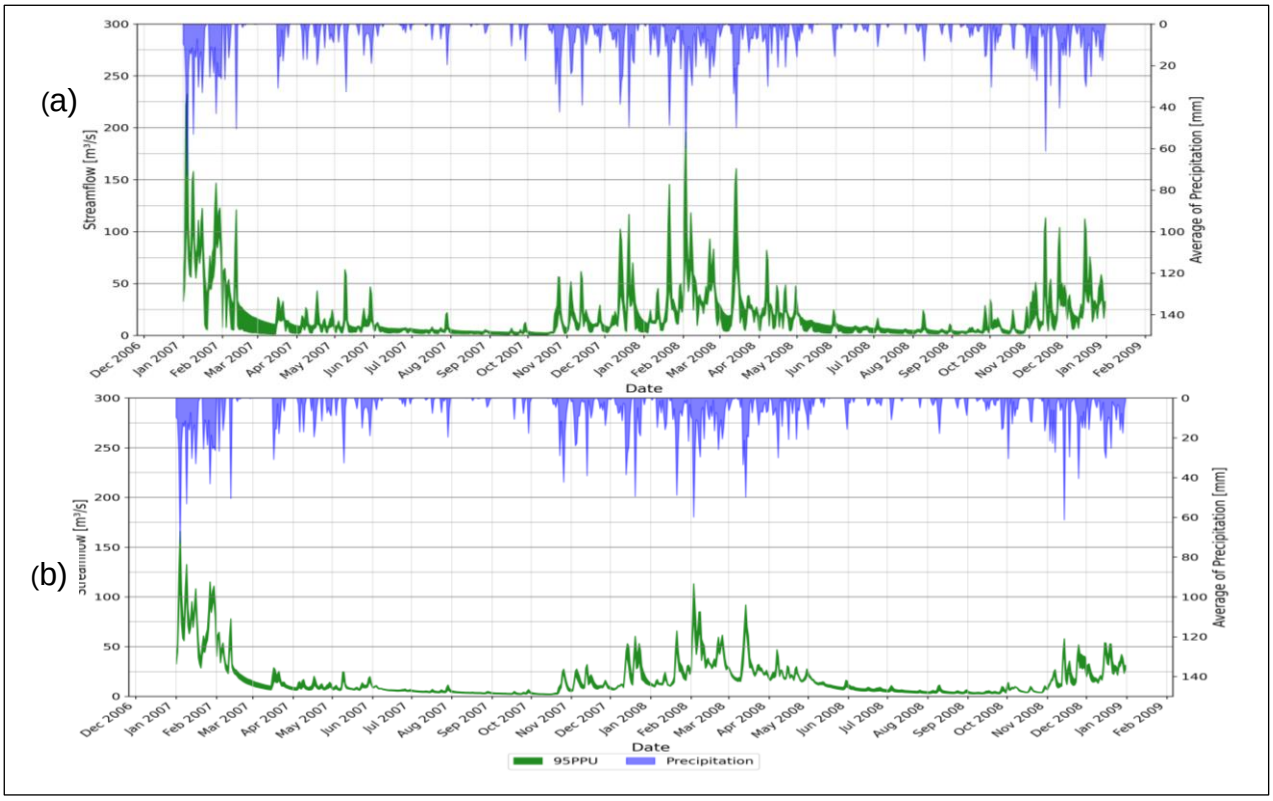

Figure 5. Uncertainty band for channel flow. (a) KF from 1 to 100. (b) KF from 10 to 100.

The present study addresses this gap by demonstrating that a regional anisotropy ratio (KF) of 15 provides the most accurate representation of lateral flow within the Pedro do Rio watershed. Although higher anisotropy might be expected given the dominance of shallow, low-permeability Cambisols, the resulting value appears to reflect a balance between contrasting factors. The significant forest cover (~62%) may improve surface soil structure and infiltration capacity, while the presence of deeper, better-drained Latosols could also

moderate the basin's regional anisotropic response. These combined influences may help explain the intermediate KF value observed. Nonetheless, further studies are needed to better understand how soil heterogeneity, vegetation, and topography interact to control anisotropy in tropical watersheds.

This conclusion is drawn under the specific infiltration and precipitation conditions supplied to the model. Nevertheless, it is important to highlight that variations in input data or boundary conditions could potentially shift this improved anisotropy ratio. This finding reinforces the dynamic and context-dependent nature of hydrological model calibration, emphasizing the necessity for continual refinement and adaptation in hydrological modeling practices to accommodate changing environmental and operational scenarios.

Given that anisotropy and soil stratification are the main drivers of lateral soil flow (SINAI & DIRKSEN, 2006), their adjustment reduces uncertainty about flows within the porous media, allowing for a more accurate representation of these flows. Following the logic of Yeh and Tsai (2018), a factor of 15 indicates considerably porous soil. Another factor to consider is that, in a mountainous region, water reaching the bedrock may only flow laterally, leading to a significant increase in lateral flow.

The study's findings are significant but limited by their reliance on input data and boundary condition quality. Key infiltration and precipitation parameters were essential in determining an optimal anisotropy ratio of 15 for the Pedro do Rio watershed, yet variations in these inputs could affect results, requiring further research to assess their influence on model calibration and anisotropy values. The focus on a single watershed restricts the generalizability of the findings, emphasizing the need to analyze diverse watersheds to strengthen applicability. Future studies should also investigate the interactions between anisotropic hydraulic conductivity and other hydraulic parameters to better understand their combined effects on lateral flow dynamics and model performance.

5. CONCLUSIONS

This study addressed the identified research gap by quantifying the sensitivity and uncertainty of hydraulic conductivity anisotropy in the MOHID-Land model, specifically for the Pedro do Rio watershed. The analysis revealed that an optimal anisotropy ratio of 15 effectively captured the lateral flow dynamics characteristic of this steep, mountainous terrain, confirming the hypothesis that lateral flow plays a significant hydrological role in this

region. These findings directly support the assumptions made in the introduction regarding the critical impact of anisotropy on flow patterns in sloped areas of the Atlantic Forest biome.

Despite these advancements, limitations related to input data quality, boundary conditions, and the exclusive focus on a single watershed were acknowledged. While the study provided a robust framework for calibrating anisotropy in MOHID-Land model, its generalizability could be enhanced by extending the analysis to watersheds. Additionally, the interactions between anisotropy and other hydraulic parameters should be further investigated to refine model predictions under varying conditions.

The findings contribute not only to advancing hydrological modeling in the Pedro do Rio watershed but also to establishing a methodology applicable to similar environments, thereby supporting broader efforts in watershed management and conservation.

REFERENCES

ABBASPOUR, K. C. SWAT-CUP: SWAT calibration and uncertainty programs – a user manual. **Eawag: Dübendorf, Switzerland**, p. 16-70, 2015.

ALLEN, R. G et al. Crop evapotranspiration-Guidelines for computing crop water requirements-FAO Irrigation and drainage 56. **Fao, Rome**, v. 300, n. 9, p. D05109, 1998.

ARAÚJO, L. M. N. **Identificação de padrões hidrológicos de precipitação e de umidade do solo na bacia hidrográfica do rio Piabanha/RJ. 2016**. Tese (Doutorado em Engenharia Civil), Universidade Federal do Rio de Janeiro, Rio de Janeiro. 2016.

BECK-BROICHSITTER, S. et al. Anisotropy of soil water diffusivity of hillslope soil under spruce forest derived by X-ray CT and lab experiments. Environmental Earth Sciences, v. 81, n. 18, p. 457, 2022.

COSTA, D. A. et al. From monitoring and modeling to management: How to improve water quality in Brazilian rivers? A case study: Piabanha River Watershed. **Water**, v. 13, n. 2, p. 176, 2021.

COSTA, D.; BAYISSA, Y.; SALES, D.; DIAS, R. M. M. S.; LUGON JUNIOR, J.; SILVA NETO, A. J.; SRINIVASAN, R. Spatial and temporal variability of precipitation in a mountainous watershed using weighted interpolation by distance and elevation. In: **XII Encontro de Sustentabilidade em Projeto**, Belo Horizonte, v. 12. p. 602-610, 2024.

HERSBACH, H. et al. The ERA5 global reanalysis. **Quarterly Journal of the Royal Meteorological Society**. 2020.

HORN, Rainer et al. Soil type and land use effects on tensorial properties of saturated hydraulic conductivity in northern Germany. **European Journal of Soil Science**, v. 71, n. 2, p. 179-189, 2020.

MASKEY, S. HyKit: **A Tool for Grid-Based Interpolation of Hydrological Variables**. User's Guide (Version 1.3), 1-6, 2013.

MORIASI, D. N. et al. Hydrologic and water quality models: Performance measures and evaluation criteria. **Transactions of the ASABE**, v. 58, n. 6, p. 1763-1785, 2015.

MUALEM, Y. A new model for predicting the hydraulic conductivity of unsaturated porous media. **Water Resources Research**, v. 12, n. 3, p. 513-522, 1976.

OLIVEIRA, A. R. et al. Sensitivity analysis of the MOHID-Land hydrological model: a case study of the ulla river basin. **Water**, v. 12, n. 11, p. 3258, 2020.

RICHARDS, Lorenzo Adolph. Capillary conduction of liquids through porous mediums. **Physics**, v. 1, n. 5, p. 318-333, 1931.

SALES, D. S.; LUGON JUNIOR, J.; COSTA, D. A.; SILVA NETO, A. J. **Timeseries Error and Uncertainty Analyzer** (Version 2.0.0) [Computer software]. 2024. https://github.com/dhiegosales/Timeseries-Error-and-Uncertainty-Analyzer.

SALES, D. S. et al. Enhancing hydrological modeling accuracy: integrating EMBRAPA soil texture data with Rosetta model input parameters using the MOHID SOIL TOOL. In: **Anais do Encontro Nacional de Modelagem Computacional e Encontro de Ciência e Tecnologia de Materiais**. Anais, Ilhéus (BA), 2024.

SINAI, G.; DIRKSEN, C. Experimental evidence of lateral flow in unsaturated homogeneous isotropic sloping soil due to rainfall. **Water resources research**, v. 42, n. 12, 2006.

SOUZA J. R. et al. Reconstructing three decades of land use and land cover changes in brazilian biomes with landsat archive and earth engine. **Remote Sensing**, v. 12, n. 17, p. 2735, 2020.

USOWICZ, B.; LIPIEC, J. Spatial variability of saturated hydraulic conductivity and its links with other soil properties at the regional scale. **Scientific Reports**, v. 11, n. 1, p. 8293, 2021.

VALERIANO, M. M.; ROSSETTI, D. F. Topodata: Brazilian full coverage refinement of SRTM data. **Applied Geography**, v. 32, n. 2, p. 300-309, 2012.

VAN GENUCHTEN, M. A closed-form equation for predicting the hydraulic conductivity of unsaturated soils. **Soil science society of America journal**, v. 44, n. 5, p. 892-898, 1980.

VASQUES, G. M.; COELHO, M. R.; DART, R. O.; CINTRA, L. C.; BACA, J. F. M. Soil Clay, Silt and Sand Content Maps for Brazil at 0-5, 5-15, 15-30, 30-60, 60-100 and 100-200 cm Depth Intervals with 90m Spatial Resolution. **Embrapa Solos**, Rio de Janeiro, Brazil. 2021a.

VASQUES, G. M.; COELHO, M. R.; DART, R. O.; CINTRA, L. C.; BACA, J. F. M., Soil Bulk Density Maps for Brazil at 0-5, 5-15, 15-30, 30-60, 60-100 and 100-200 cm Depth Intervals with 90m Spatial Resolution. **Embrapa Solos**, Rio de Janeiro, Brazil. 2021b.

VILLAS-BOAS, M. D. **Ferramentas para avaliação da rede de monitoramento de**

qualidade de água da bacia do rio Piabanha – RJ com base em redes neurais e modelagem hidrológica. Tese (Doutorado em Engenharia Civil), Universidade Federal do Rio de Janeiro, Rio de Janeiro. 2018.

VILLAS-BOAS, M. D. et al. Assessment of the water quality monitoring network of the Piabanha River experimental watersheds in Rio de Janeiro, Brazil, using autoassociative neural networks. **Environmental monitoring and assessment**, v. 189, p. 1-15, 2017.

WOESSNER, W. W.; POETER, E. P. Hydrogeologic properties of earth materials and principles of groundwater flow. **Groundwater Project**, 2020.

YEH, Hsin-Fu; TSAI, Yi-Jin. Analyzing the effect of soil hydraulic conductivity anisotropy on slope stability using a coupled hydromechanical framework. **Water**, v. 10, n. 7, p. 905, 2018.

ZHANG, Y.; SCHAAP, M. G. Weighted recalibration of the Rosetta pedotransfer model with improved estimates of hydraulic parameter distributions and summary statistics (Rosetta3). **Journal of Hydrology**, v. 547, p. 39-53, 2017.